ACTA TECHNICA CORVINIENSIS – Bulletin of Engineering | e–ISSN: 2067 – 3809
Tome XVIII [2025] | Fascicule 1 [January – March]

[1,2.] A.A ADEDIRAN, [3] A.S. OLABISI, [1.] C.I. MADUEKE, [4,5.] J.T. STEPHEN, [4] I. ADEIZA, [4] I. NWAMADI, [4] M. EBENEZER

MODELING OF WEAR PARAMETERS OF ALUMINIUM METAL MATRIX COMPOSITES REINFORCED WITH ALUMINA, WASTE CANS, AND Si-BASED REFRACTORY COMPOUNDS OF BAMBOO LEAVES

[1.] Materials and Metallurgical Engineering Department, Faculty of Engineering, Federal University Oye-Ekiti, P.M.B 373, Oye-Ekiti, Ekiti State, NIGERIA
[2.] Mechanical Engineering Science, University of Johannesburg, SOUTH AFRICA
[3.] Mechanical Engineering Department, College of Engineering, Williams Tubman University, LIBERIA
[4.] Mechanical and Mechatronics Engineering Department, Landmark University, Omu-Aran, Kwara State, NIGERIA
[5.] Mechanical Engineering Department, Ekiti State University, Ado-Ekiti, NIGERIA

Abstract: This study investigates the wear properties of Al-Mg-Si - based composites and various reinforcing materials (such as alumina and silicon-based refractory compounds produced from bamboo leaves). Statistical methods, including analysis of variance (ANOVA) were used to evaluate the significance and effect of experimental wear and filler content. From the results obtained, the specific wear rate was lowest at 0.002349 $mm^2/g{\cdot}mm^3$ for the D hybrid composite at a load of 150 N and a sliding time of 360 s. The effectiveness of the prediction model was evaluated by P value and F value, which revealed the adequacy of the model in predicting the response. It was noted that the numerical optimization determines the best location according to maximum demand. The results showed that wear varied with load and time, and the study confirmed that the oxide content in the reinforcement material helped in reducing wear.
Keywords: modeling, wear, aluminium, matrix, composite, reinforcement, bamboo leaves

INTRODUCTION

There is interest in investigating low-cost options for the production of aluminum matrix composites (AMCs) that can still maintain high levels of performance in service (Saeed, Imran, & Lee, 2022). AMC is a versatile metal matrix composite due to many factors such as ease of processing, low cost of the aluminum matrix compared to other competing metal matrices (copper, titanium, magnesium), good combination of body and all products, good hot performance and thermal management ability, excellent tribological properties and reasonable corrosion resistance (Christy, Murugan, & Kumar, 2010) (Alanene & Aluko, 2012) (Alaneme A. A., 2012).

The cost of aluminum metal matrix composites (AMMC) remains high, limiting its use. Using cheap energy sources such as natural materials can reduce the overall cost of AMMCs and also make them more efficient (Marin, et al., 2012). Many efforts have been made to use commercial and agricultural wastes as supplementary materials to find a low-cost option for AMMC production (Prakash, Kanagaraj, & Gopal, 2015). In this context, many researchers have tried to use waste materials such as garbage bags, rice husk ash (RHA), coconut shell ash, palm shell ash, groundnut shell (GSA), bamboo leaves, etc. as motivational data. Agricultural waste ash contains high amounts of silicon dioxide (SiO_2) and is dispersed with other elements such as Al_2O_3, Fe_2O_3, CaO, MgO, and C (Aigbodion, Hassan, Dauda, & Mohammed, 2011) (Allwyn, Mohamed, Dinaharan, & David, 2015) (Ankesh, Kanhaiya, Suman, & Siva , 2016) (Oladele & Okoro, 2016) (Alaneme, Eze, & Bodunrin, 2015) (Cocina, Morales, Santos, Savastano, & Moises, 2011). Aluminum production is quite energy-intensive because its production is based on the electrolytic reduction process involving high currents (Zhang, et al., 2016). It is estimated that the electricity used during production can account for 20% to 40% of production costs (Adediran, Alaneme, Oladele, & Akinlabi, 2018).

MATERIALS AND METHODS

AA 6063 (Al-Mg-Si), the main material of this study, was obtained in ingot form from a local supplier. The reinforcement materials used in this study are alumina (Al_2O_3) with a particle size of 30 µm and silicon-based refractory material (SBRC) obtained from bamboo leaves (BLA) with a particle size greater than 60 µm.

Magnesium is used to increase the wettability of the substrate and reinforcement.

Table 1: Sample designation

Samples	Constituents
A	Waste Can
B	3wt.% BLA + 7 wt.% Al_2O_3
C	5wt.% SiC + 5 wt.% Al_2O_3
D	10 wt.% SiC

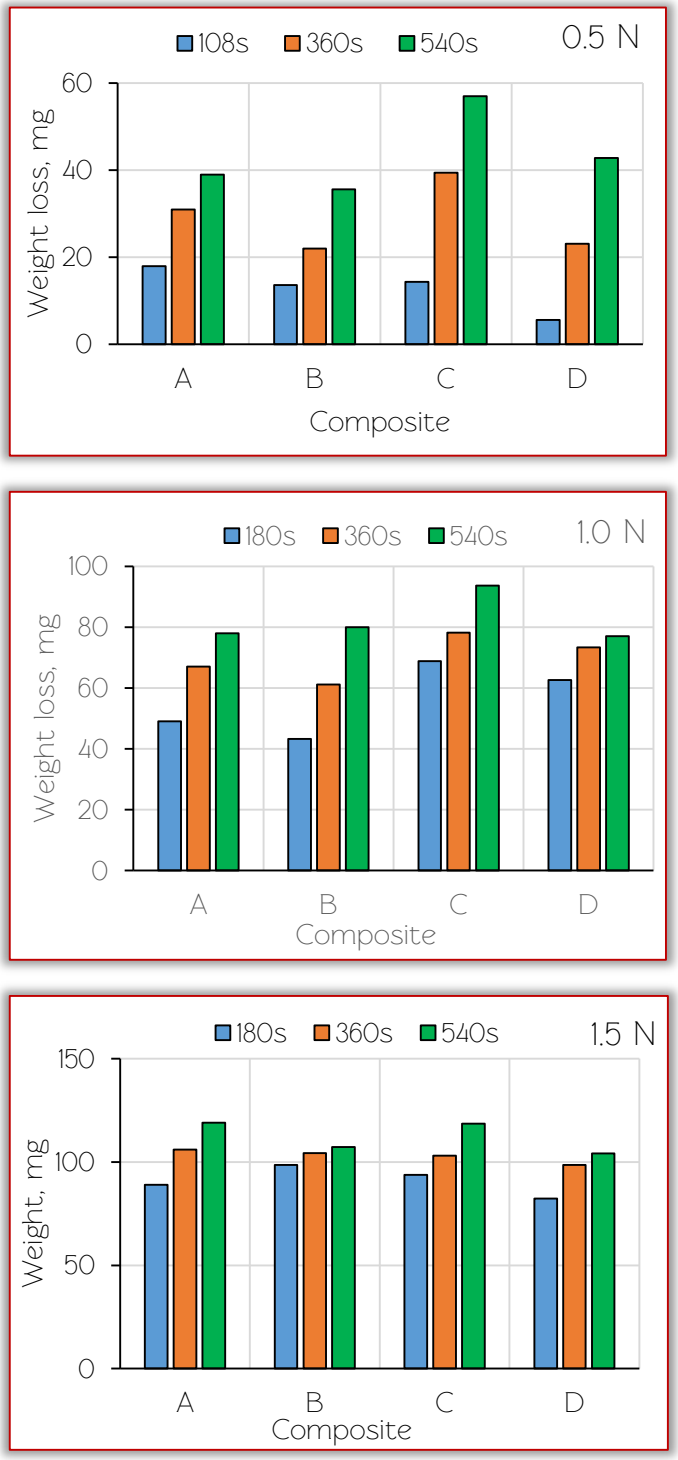

Figure 1: Effect of variation in applied load (0.5, 1.0, and 1.5 N) and sliding time (180 s, 360 s, and 540 s) on weight loss of developed compositions

The synthetic method to produce SBRC has been described previously (Adediran, Alaneme, Oladele, & Akinlabi, 2018). Table 1 shows the samples nomenclature and constituents of each composite.

RESULTS AND DISCUSSION

Effect of sliding time and applied load on the weight loss

Compared to an unreinforced alloy, the sliding wear resistance of an aluminum alloy (Al-Mg-Si) is improved by adding agricultural particles. The impact of the sliding time and applied force on the proportion of agro-particles in aluminum alloy were investigated. Figure 1 illustrates the correlation between the weight loss of the reinforced samples and the base alloy samples, considering the sliding time and the applied load. It can be seen from the figure that the unreinforced matrix alloy loses more weight than the reinforced samples under the same applied loading conditions. Additionally, it is noted that when applied stress and sliding time are increased, so does the weight loss of both compositions. This may be attributed to the limited infiltration of agricultural particles into the surface of the test sample when a smaller force is applied, leading to less material removal. The level of penetration rises proportionally with an increase in the applied load. Consequently, when the applied stress is higher, there is a greater amount of material removed from the test sample (Prasanna, Sadashivappa, Puttappa, & Basavarajappa, 2006). According to a paper by Patel *et al.* (Patel, Sahu, & Singh, 2020), the use of agro or ceramic reinforcement can slow down the progression of wear from a mild to a severe state by either increasing the applied load or the sliding time. The study suggests that including agro-reinforcement slows the progression from mild to severe wear.

Effect of sliding time and applied load on the wear rate

The influence of the applied loads and sliding time on the wear rate of produced composites is illustrated in Figure 2. It is observed that the wear rate increases with an increase in applied load. This is because of the rise in weight loss of the composites with higher applied loads and sliding time [18]. In addition, when the normal load increases frictional heat builds up at the contact surface and consequently the strength of materials diminishes (Alanene & Aluko, 2012). The wear rate of agro-reinforced aluminum is lower than that of unreinforced aluminum because of the reinforcement's high toughness and excellent bonding between the reinforcement and the aluminum matrix composite.

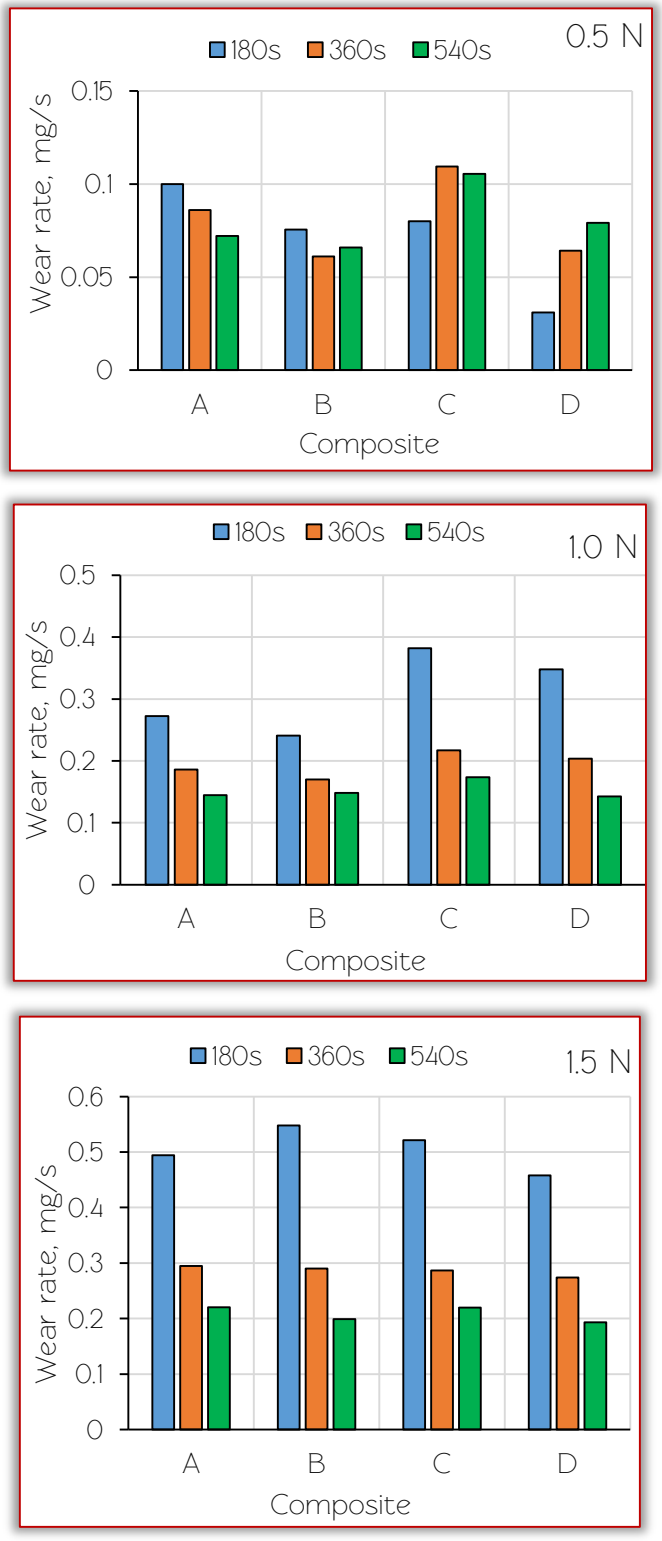

Figure 2: Effect of variation in applied load (0.5, 1.0, and 1.5 N) and sliding time (180 s, 360 s, and 540 s) on wear rate of developed compositions

Effect of sliding time and applied load on the specific wear rate

Figure 3 displays the specific wear rate for samples of unreinforced alloy and agro-particle reinforcement plotted against sliding time at various applied loads (0.5 N, 1.0 N, and 1.5 N). The main variables influencing the wear of composites during sliding are the period that the composite is in motion and the applied load. Studies have demonstrated that there is a crucial transition load when the rate of wear rises significantly (Manivannan, Ranganathan, Gopalakannan, & Suresh, 2018). As the applied load is raised from 0.5 N to 1.5 N, Figure 3 shows that the specific wear rate of the unreinforced alloy increases with an increase in sliding time.

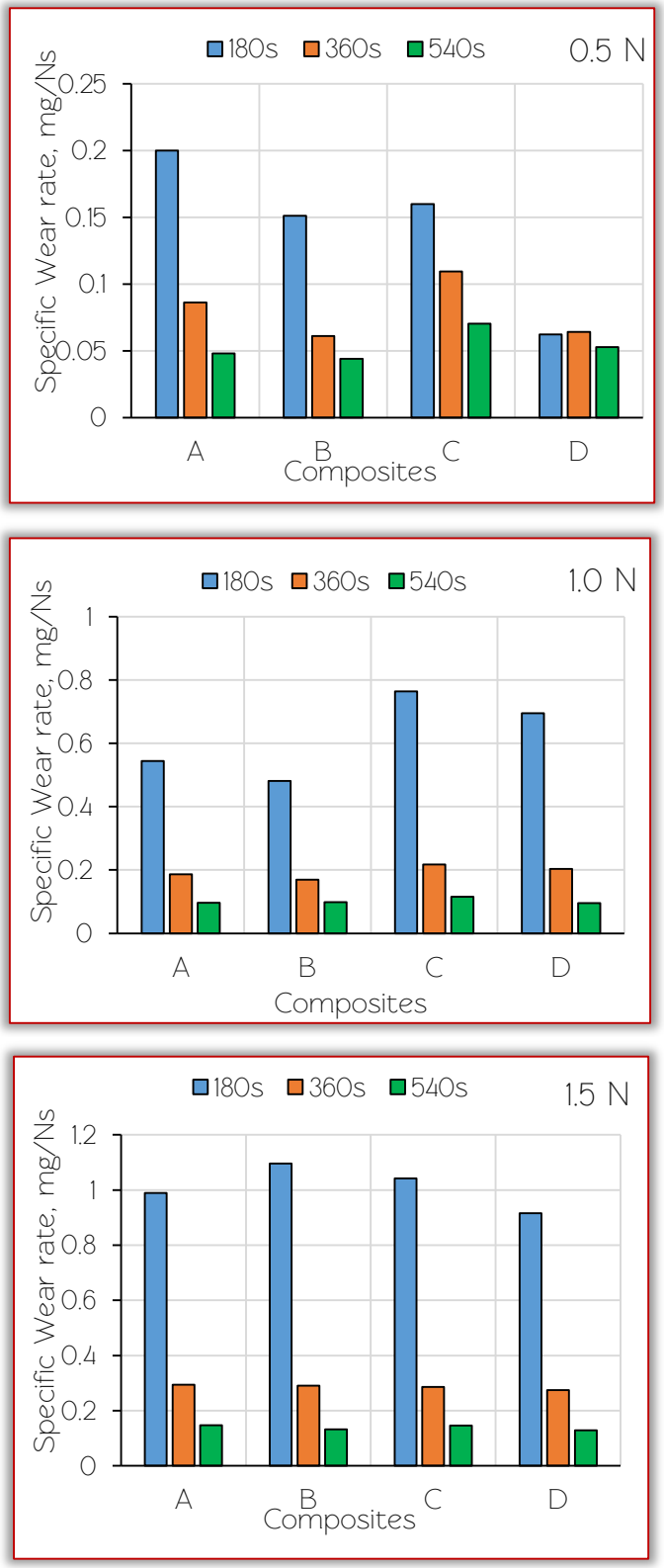

Figure 3: Effect of variation in applied load (0.5, 1.0, and 1.5 N) and sliding time (180 s, 360 s, and 540 s) on the specific wear rate of developed compositions

The degradation of wear resistance with increased load is the cause of the rise in specific wear rates. As the sliding time rises at all applied loads, Figure 3 shows that the specific

wear rate of the reinforced alloy samples is relatively low compared to the specific wear rate of the unreinforced alloy due to the toughness of the incorporated agro particles. According to Pradhan *et al.* (Pradhan, Barman, Sahoo, & Sutradhar, 2017), the agro-particles reduce the amount of disintegration and dispersing by preventing the slider from cutting through the surface of the reinforced samples. Moreover, the agro-particles strengthen the matrix alloy's toughness and serve as load-bearing particles in the unreinforced matrix alloy, protecting the soft matrix from sliding wear.

Statistical analysis, modelling and optimization of wear properties and parameters

The accuracy of the developed prediction model was evaluated by analysis of variance. Analysis of variance is effective in determining the adequacy of statistical data, its importance, and the appropriate input of multiple and variable responses. It also evaluates the results of negative and filler content tests on the product of the test. A relationship has been established between the properties that improve the properties of metal matrix composites and different reactions (wear properties). The results of the analysis of variance and a summary of the fit statistics are described in Tables 2, 3, and 4 respectively.

Table 2: ANOVA and summary of fit statistics for response 1 (Wear Loss)

Source	Sum of Squares	df	Mean Square	F-value	p-value	
Model	0.1070	5	0.0214	31.92	< 0.0001	significant
A-Load	0.0918	1	0.0918	136.97	< 0.0001	
B-Time	0.0154	1	0.0154	22.99	0.0003	
C-composition	0.0026	3	0.0009	1.30	0.3143	
Residual	0.0094	14	0.0007			
Lack of Fit	0.0094	13	0.0007			
Pure Error	0.0000	1	0.0000			
Cor Total	0.1163	19				

Table 3: ANOVA and summary of fit statistics for response 2 (Wear Rate)

Source	Sum of Squares	df	Mean Square	F-value	p-value	
Model	0.0440	5	0.0088	6.87	0.0020	significant
A-Load	0.0007	1	0.0007	0.5105	0.4867	
B-Time	0.0103	1	0.0103	8.02	0.0133	
C-composition	0.0302	3	0.0101	7.87	0.0026	
Residual	0.0179	14	0.0013			
Lack of Fit	0.0179	13	0.0014			
Pure Error	0.0000	1	0.0000			
Cor Total	0.0619	19				

Table 4: ANOVA and summary of fit statistics for response 3 (Specific wear rate)

Source	Sum of Squares	df	Mean Square	F-value	p-value	
Model	0.0159	5	0.0032	6.75	0.0021	significant
A-Load	0.0002	1	0.0002	0.4839	0.4981	
B-Time	0.0038	1	0.0038	7.96	0.0136	
C-composition	0.0109	3	0.0036	7.69	0.0028	
Residual	0.0066	14	0.0005			
Lack of Fit	0.0066	13	0.0005			
Pure Error	0.0000	1	0.0000			
Cor Total	0.0226	19				

Table 5: The constraints for the model

Name	Goal	Lower Limit	Upper Limit	Lower Weight	Upper Weight	Importance
A: Load	is in range	50	150	1	1	3
B: Time	is in range	180	540	1	1	3
C: composition	is in range	A	D	1	1	3
mass loss	none	0.0748	0.3449	1	1	3
WR	none	0.00178	0.1476	1	1	3
SWR	none	0.0005	0.0890	1	1	3

Table 6: Solutions for four combinations of categoric factor levels

No.	Load	Time	Comp.	mass loss	WR	SWR	Desirability	
1	105.219	396.553	D	0.061	0.007	0.002	1.000	Selected
2	100.000	360.000	A	0.061	0.007	0.003	1.000	
3	50.000	540.000	B	0.037	0.001	0.000	1.000	
4	150.000	540.000	B	0.123	0.001	0.000	1.000	
5	50.000	180.000	D	0.015	0.003	0.001	1.000	

The P values (significant values) obtained for each response variable for each factor were below 0.0500, indicating that the model was statistically significant. Values above 0.1000 indicate that the model term is not significant. The F value of each variable is also significant, which is a good indication that the input material has a positive effect on the reaction (Nwaeju, Edoziuno, Adediran, Nnuka , & Akinola, 2021) (Adzor, Nwaeju, & Edoziuno, 2021). Therefore, the ratio of response variables is greater than 4, which clearly indicates that the design is sufficient to reach the design point. Tables 5 and 6 displayed the solution data for the model.

Graphical analysis of model

Design-Expert software provides a variety of diagrams to help explain model fit. Use diagnostic plans and drawing models to identify and interpret assembly patterns. The predicted versus modeled plot in Figure 4A-C show actual response values compared to the predicted response and helps identify observations that

the model may not have predicted. The fact that the data points are distributed around a 45-degree line shows that the model is sufficient to predict the response (Edoziuno, et al., 2021) (Odoni, Edoziuno, Nwaeju, & Akaluzia, 2020).

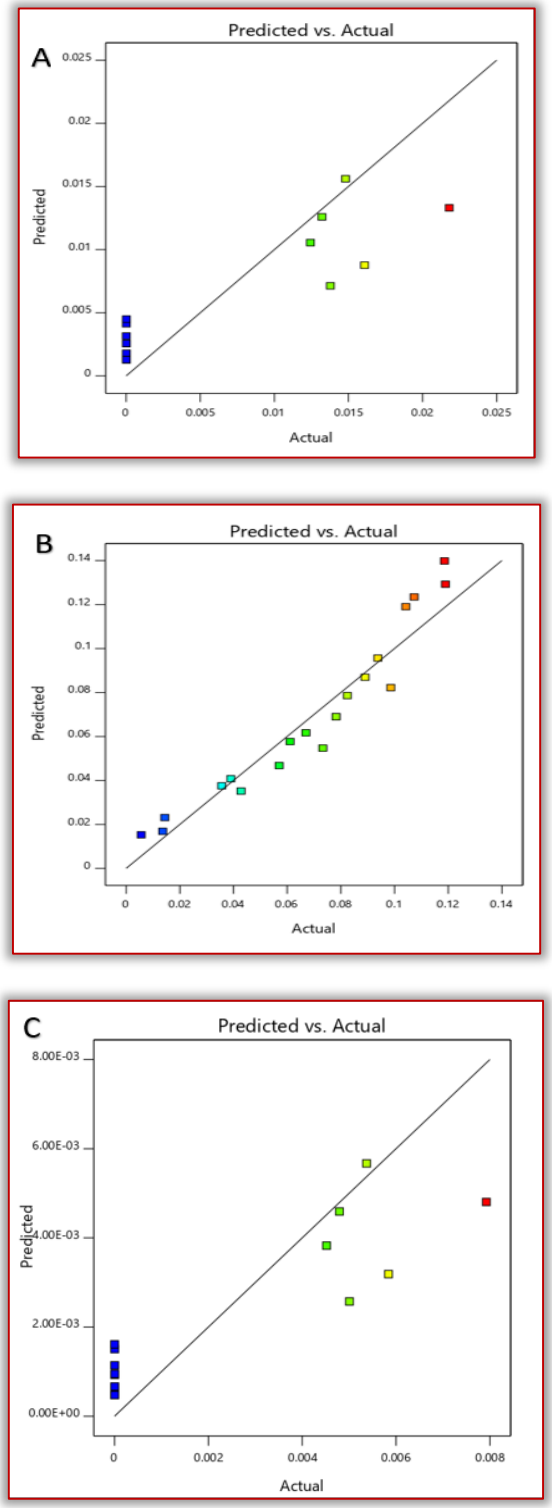

Figure 4. Standard prediction methods versus actual design values for (A) wear loss, (B) wear rate, and (C) specific wear rate.

The main modeling tools for response modeling are 3D and contour plots. Contour plots provide a two-dimensional (2D) representation of reaction variables plotted against a combination of numbers and show the relationship between the reaction and the number (Odoni, Edoziuno, Nwaeju, & Akaluzia, 2020). 3D surface map enables the projection of the contour map by adding images to color and contour points. Figures 5A–C feature an interactive 3D surface showing the interaction between factors and response variables at the categorical factor level (Odoni, Edoziuno, Nwaeju, & Akaluzia, 2020).

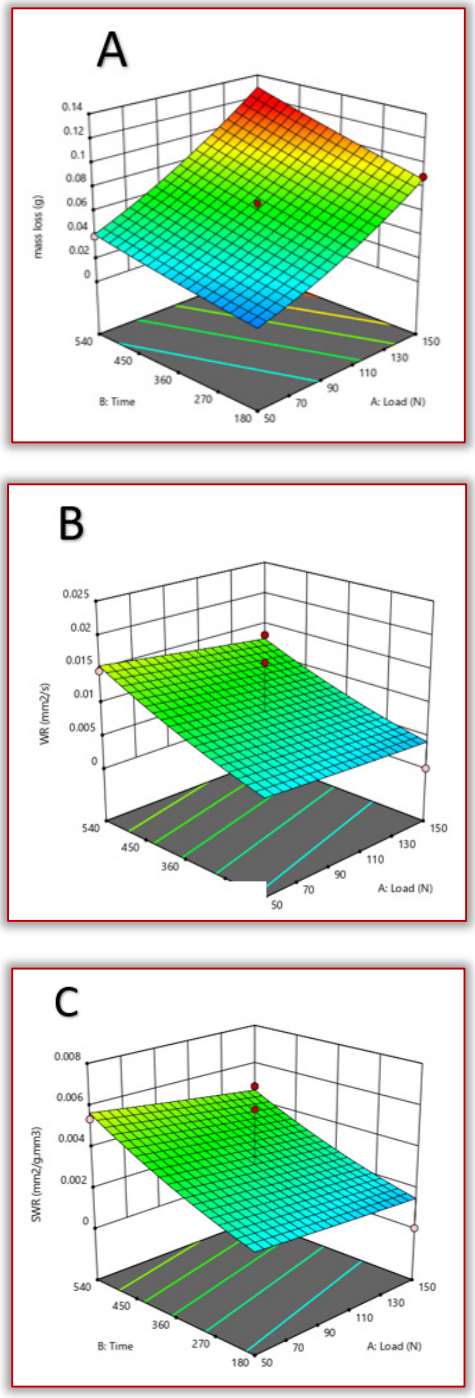

Figure 5. Interactive 3D surface model plot of (A) wear loss, (B) wear rate, and (C) specific wear rate for the design.

Interaction occurs when the response varies according to the configuration of two parameters (load and time) (Edoziuno, et al., 2020). This interaction is represented by two parallel lines, showing that the effect of one depends on the level of the other. The impact plots shown in Figure 6A-C are used to compare

the effects of each factor on a specific location in the design space. The answer is plotted by changing only one factor within its range, keeping all other factors constant. By default, Design-Expert puts the reference point at the center of everything (coded as 0). This can be changed anywhere using the feature (probably the best workaround). The slope or curvature in a curve indicates that the response is sensitive to values.

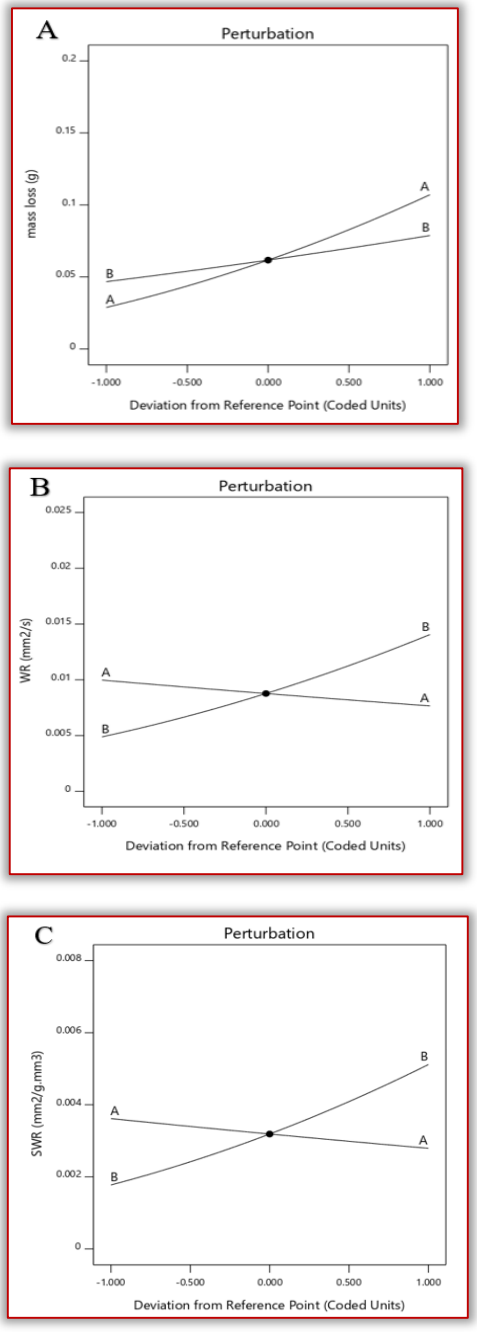

Figure 6. Perturbation plots of (A) wear loss, (B) wear rate, and (C) specific wear rate.

Parametric optimization solution

Tables 5 and 6 describe the process of using constraints and critical steps used to determine the optimal location and solution for the optimal mathematical procedure. The best solution that meets the criteria determined from the numerical optimization report is selected as the optimal solution. This is usually the solution with the highest score, indicating the range of results obtained.

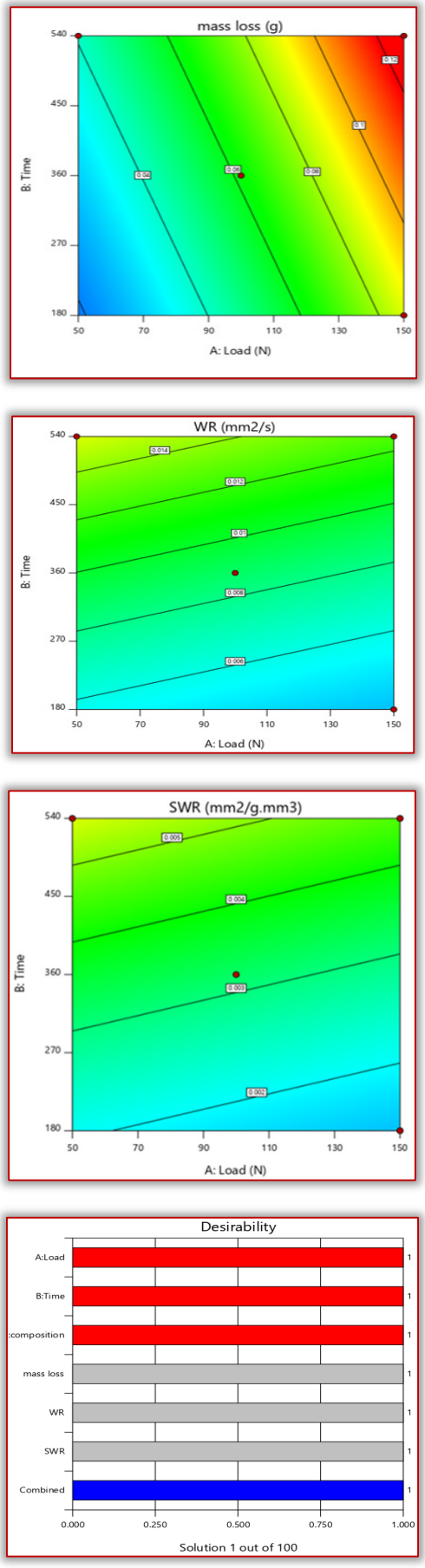

Figure 7. Desirability of contour plots and numerical optimization results.

Numerical optimization methods are set to optimize one or more targets that can be used for different reactions. Goal types during numerical optimization include: maximize, minimize, objective, within range, none (field only), and set to any value (item only). The ideal solution is represented using diagrams, strata plans and demand plans (Figures 7 and 8). The overlay shows the "sweet spot" where all responses are consistent with the model. By default, a profitable issue is displayed in yellow, and a negative issue is displayed in gray.

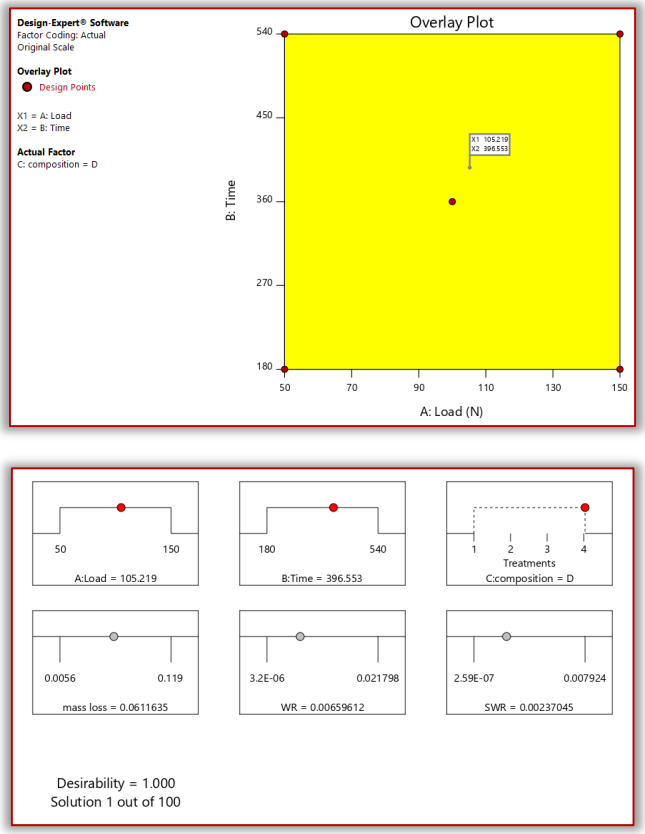

Figure 8. A layer showing the numerical optimization solution.

CONCLUSION

The study effectively demonstrates that AA 6063 hybrid composites' wear performance is significantly influenced by reinforcement types, load and time. With the lowest specific wear rate recorded at 0.002349 mm²/g·mm³ for the D hybrid composite under optimal conditions, the findings confirm the effectiveness of the chosen reinforcements in reducing wear loss. Statistical and graphical analyses reveal critical interactions between factors and highlight optimal settings for improved performance. These results offer valuable guidance for optimizing composite materials to achieve enhanced wear resistance.

References

[1] Adediran, A. A., Alaneme, K. K., Oladele, I. O., & Akinlabi, E. T. Processing and structural characterization of Si-based carbothermal derivatives of rice husk, Cogent Engineering, 2018

[2] Adzor, S. A., Nwaeju, C. C., & Edoziuno, F. O. Optimization of tensile strength for heat treated micro-alloyed steel weldment. Materials Today Proceeding, 2021.

[3] Aigbodion, V. S., Hassan, S. B., Dauda, E. T., & Mohammed, R. A. Experimental study of aging behavior of Al—Cu—Mg/bagasse ash particulate composites. Tribology in Industry, 33, 28–35, 2011.

[4] Alaneme, A. A. Influence of thermo-mechanical treatment on the tensile behaviour and cnt evaluated fracture toughness of Borax premixed SiC p reinforced AA 6063 composites. International Journal of Mechanical and Materials Engineering, 7(1), 96-100, 2012.

[5] Alaneme, K. K., Eze, H. I., & Bodunrin, M. O. Corrosion behavior of groundnut shell ash and silicon carbide hybrid reinforced Ag—Mg—Si alloy matrix composites in 3.5% NaCl and 0.3M H2SO4 solutions. Leonardo Electronic Journal of Practices and Technologies, 26, 129-146, 2015.

[6] Alanene, K. K., & Aluko, A. O. Cost-effective production of aluminum matrix composites for high-performance applications. Scientia Iranica, Transactions A: Civil Engineering Elsevier, 19(4), 992-996, 2012.

[7] Aliyu, S. J., Adekanye, T. A., Adediran, A. A., & Ogundipe, O. L. Influence of micro-addition of lanthanum on grain characteristics, mechanical properties, and corrosion behavior of CuAlNiMnLa shape memory alloy. Research on Engineering Structures and Materials, 2024

[8] Aliyu, S. J., Adekanye, T. A., Adediran, A. A., Ikubanni, P. P., & Ogundipe, O. L. A Review on the Effect of Rare Metals Additions on the Mechanical and Damping Properties of CuAlNi Shape Memory Alloys. 2024 International Conference on Science, Engineering and Business for Driving Sustainable Development Goals (SEB4SDG), 2024

[9] Allwyn, K., Mohamed, S. N., Dinaharan, I. J., & David, R. S. Production and characterization of rice husk ash particulate reinforced AA6061 aluminum alloy composites by compocasting. Transactions of Nonferrous Metals Society of China, 25, 683-691, 2015.

[10] Ankesh, K., Kanhaiya, K., Suman, S., & Siva , S. R. Study of physical, mechanical, and machinability properties of aluminum metal matrix composite reinforced with coconut shell ash particulates. Imperial Journal of Interdisciplinary Research, 2, 151-157, 2016.

[11] Asaduzzaman, C., Muhammad, N. D., & Lutfar, R. M. The effect of sliding speed and normal load on friction and wear property of aluminum. International Journal of Mechanical & Mechatronics Engineering IJMME-IJENS, 2011.

[12] Christy, T. V., Murugan, N., & Kumar, S. A Comparative Study on the Microstructures and Mechanical Properties of Al 6061 Alloy and the MMC Al 6061/TiB2/12P. Journal of Minerals and Materials Characterization and Engineering, 57-65, 2010.

[13] Cocina, E. V., Morales, E. V., Santos, S. F., Savastano, H. J., & Moises, F. Pozzolanic behavior of bamboo leaf ash: Characterization and determination of the kinetic parameters. Cement & Concrete Composites, 33, 68–73, 2011.

[14] Edoziuno, F. O., Akaluzia, R. O., Adediran, A. A., Odoni, B. U., Edibo, S., Adesina, O. S., & Edoziuno, F. Tribological Performance Evaluation of Hardwood Charcoal Powder Reinforced Polyester Resin with Response Surface Modelling and Optimization. Tribology in Industry, 43, 574-578, 2021

[15] Edoziuno, F., Adediran, A. A., Udoni, B. U., Akinwekomi, A. D., Adesina, O. S., & Oki, M. Optimization and development of predictive models for the corrosion inhibition of mild steel in sulphuric acid by methyl-5-benzoyl-2-benzimidazole carbamate (mebendazole). Cogent Engineering, 7(1), 1-19, 2020.

[16] Manivannan, I., Ranganathan, S., Gopalakannan, S., & Suresh, S. Mechanical Properties and Tribological Behavior of Al6061–SiC–Gr Self-Lubricating

Hybrid Nanocomposites. Transactions of the Indian Institute of Metals, 71(18), 1897–1911, 2018.

[17] Marin, E., Lekka, M., Andreatta, F., Itskos, G., Moutsatsou, A., Koukouzas, N., & Kouloumbi, N. Electrochemical study of aluminum-fly ash composites obtained by powder metallurgy. Materials Characterization, 69, 16–30, 2012.

[18] Nwaeju, C. C., Edoziuno, F. O., Adediran, A. A., Nnuka , E. E., & Akinola, E. T. Development of regression models to predict and optimize the composition and the mechanical properties of aluminium bronze alloy. Advances in Materials and Processing Technologies, 1-18, 2021.

[19] Odoni, B. U., Edoziuno, F. O., Nwaeju, C. C., & Akaluzia, R. O. Experimental analysis, predictive modelling and optimization of somephysical and mechanical properties of aluminium 6063 alloy basedcomposites reinforced with corn cob ash . Journal Of Materials And Engineering Structures, 451-465, 2020.

[20] Oladele, I. O., & Okoro, A. M. The effect of palm kernel shell ash on the mechanical properties of as-cast aluminum alloy matrix composites. Leonardo Journal of Sciences, 28, 15-30, 2016.

[21] Patel, M., Sahu, S. K., & Singh, M. K. Abrasive wear behavior of SiC particulate reinforced AA5052 metal matrix composite. Materials Today: Proceedings,, (pp. 5586–5591), 2020.

[22] Pradhan, S., Barman, T. K., Sahoo, P., & Sutradhar, G. Effect of SiC weight percentage on tribological properties of Al-SiC metal matrix composites under acid environment. In Jurnal Tribologi, 13, 2017.

[23] Prakash, K. S., Kanagaraj, A., & Gopal, P. Dry sliding wear characterization of Al 6061/rock dust composite. Transactions of Nonferrous Metals Society of China,, 25, 3893–3903, 2015.

[24] Prasanna, K. M., Sadashivappa, K., Puttappa, P. G., & Basavarajappa, S. Dry Sliding Wear Behaviour of Garnet Particles Reinforced Zinc-Aluminium Alloy Metal Matrix Composites. Materials Science (Medžiagotyra, 12(3), 2006.

[25] Saeed, A., Imran, M., & Lee, J. H. Cost-effective production of aluminum matrix composites for high-performance applications. Journal of Composite Materials, 56(10), 1435-1452, 2022.

[26] Zhang, Y., Sun, M., Hong, J., Han, X., He, J., Shi, W., & Li, X. Environmental footprint of aluminum production in China. Journal of Cleaner Production, 133, 1242–1251, 2016.

ISSN: 2067-3809